Title	ALE based EFGM for Analysis of Membrane Structures with Sliding Cable (Discretization Methods and Numerical Algorithms for Differential Equations)
Author(s)	Noguchi, Hirohisa
Citation	数理解析研究所講究録 (2002), 1265: 81-88
Issue Date	2002-05
URL	http://hdl.handle.net/2433/42076
Right	
Type	Departmental Bulletin Paper
Textversion	publisher

数理解析研究所講究録 1265 巻 2002 年 81-88

ALE based EFGM for Analysis of Membrane Structures with Sliding Cable

野口裕久
慶應義塾大学システムデザイン工学科
223-8522 横浜市港北区日吉３－１４－１

Hirohisa Noguchi
Department of System Design Engineering
Keio University
3-14-1, Hiyoshi, Kohoku-ku, Yokohama
223-8522, Japan
noguchi@sd.keio.ac.jp

Summary

Many large membrane structures have been constructed in these days and large membrane structures are often tensed by cables for reinforcement of the strength. In the analysis of cable-reinforced membrane structure, there are several complicated problems, such as the fold of membrane by cable, sliding of cable on membrane surface and so on. As the finite element method can hardly to analyze these problems, authors have applied meshless method based on the element free Galerkin method to the analyses of membrane structures with cable reinforcement. In the conventional element free Galerkin method, the problem that contains discontinuous slope of displacement cannot be analyzed because of the C1 continuity condition by the moving least squares approximation. Additionally, sliding between cable and membrane surface must be considered. In this paper, the arbitrary Lagrangian-Eulerian formulation and the technique of patch are adopted in EFGM, and the proposed method is applied to the numerical example of cable-reinforced membrane structures and its validity is demonstrated.

Introduction

Recently, in order to reduce constructing cost and time, attention is paid on membrane structures and they have been used in a part of large and permanent buildings because materials for membrane have been improved. For design of membrane structure, there are three kinds of analysis to be conducted, such as form finding analysis, stress analysis and cutting analysis. In the finite element method (FEM), a different mesh is required according to the purpose of analysis, while in meshless method, a set of analyses can be conducted by using only one model, because it has no elements.

Large membrane structures are often tensed by cables for reinforcement of their strength. In order to analyze cable-reinforced membrane structures, the folded membrane by cable, which yields discontinuity of slope, has to be taken into account. Furthermore, these cables are often attached in a way that permits themselves to slide over the surface on the membrane so that the cables could find equilibrium form under the applied gravity load, wind load and so on. In the conventional finite element method, discontinuity of slope can be treated only at the boundary of elements, so re-meshing or special development of the element which allows fold is necessary to model this moving discontinuity. With these in background, authors have been developing meshless system for analyses of membrane structures.

In the meshless method, it is not necessary to subdivide analysis model into elements, therefore, the fold can be modeled at arbitrary points on membrane surface and it can move freely on the surface by

redefining the nodal arrangement. In the proposed model, a patch is defined to model the part surrounded by cables and the moving least squares approximation (MLSA) is only defined in each patch and C0 continuity condition is imposed at patch boundary by the penalty method. In order to analyze sliding cable on membrane, the interface of patch must be moved with cable. Therefore, the arbitrary Lagrangian-Eulerian (ALE) method is adopted to model the sliding cable. In ALE formulation, displacement of membrane and sliding between cable and membrane are represented as different displacement components.

Authors have applied ALE formulation to the principle of virtual work on the element free Galerkin method[1] (EFGM) in ref.[2]. In this paper, MLSA is briefly introduced and then ALE formulation including the effect of friction for the analysis of membrane structures with sliding cable is derived in detail. Finally numerical analyses are demonstrated to validate the proposed method.

Moving Least Squares Approximation

In the element free Galerkin method, MLSA is used for making approximation functions of fields. In this section the formulation of MLSA method is presented according to Belytschko et al[1]. Two-dimensional field is enough for modeling membrane structures. A component of displacement vector $\mathbf{u}(\mathbf{x})$ is approximated by a polynomial function as follows, where n is a number of terms in polynomial function. In eq.(1), a linear basis vector $\mathbf{p}$ and its coefficients vector $\mathbf{a}$ are exemplified for brevity (n=3).

$$u^h(\mathbf{x}) = \sum_{j=1}^{n} p_j(\mathbf{x}) a_j(\mathbf{x}) \equiv \mathbf{p}^T(\mathbf{x})\mathbf{a}(\mathbf{x}) \tag{1}$$

$$\mathbf{p}^T(\mathbf{x}) = (1, x, y), \quad \mathbf{a}^T(\mathbf{x}) = (a_1, a_2, a_3) \tag{2}$$

In this study, only linear basis function is used in the analyses of membrane structures. The coefficients in $\mathbf{a}(\mathbf{x})$ are determined by minimizing the following weighted functional.

$$u^h(\mathbf{x}) = \sum_{j=1}^{n} p_j(\mathbf{x}) a_j(\mathbf{x}) \equiv \mathbf{p}^T(\mathbf{x})\mathbf{a}(\mathbf{x}) \tag{3}$$

where u_I is an unknown nodal value of u at a node $\mathbf{x}_I$ and m is the number of nodes in the domain of influence. The following fourth order polynomial is adopted for a weight function, w(r), which satisfies $w(\rho) = 0$, $dw/dr(\rho) = 0$ and $d^2w/dr^2(\rho) = 0$ (ρ is a radius of the domain of influence).

$$w(r_I) = \begin{cases} 1 - 6\left(\frac{r_I}{\rho}\right)^2 + 8\left(\frac{r_I}{\rho}\right)^3 - 3\left(\frac{r_I}{\rho}\right)^4 & (0 \le r_I \le \rho) \\ 0 \quad (\rho < r_I) \end{cases} \tag{4}$$

Finally, the approximation displacement $u^h(\mathbf{x})$ can be represented by the nodal value u_I, as

$$u^h(\mathbf{x}) = \sum_{j=1}^{n} p_j(\mathbf{x}) a_j(\mathbf{x}) \equiv \mathbf{p}^T(\mathbf{x})\mathbf{a}(\mathbf{x}) \tag{5}$$

where $\phi_I(\mathbf{x})$ corresponds to a shape function in FEM.

Consideration of discontinuous slope of displacement

In this chapter, the treatment of discontinuous slope of displacement in the EFGM is briefly described. In the analysis by EFGM, continuous strain field is obtained by using MLSA for the approximation of the field function. In the analysis of structure with discontinuous gradient of displacement due to such as material discontinuity or membrane with cable, however, strain field also becomes discontinuous at the interface. Therefore the conventional EFGM cannot be applied[3].

In order to analyze the structure with discontinuous gradient of displacement, analysis model is divided into patches. Figure 1 illustrates the domains of influence near the interface of patches for analysis model of membrane with cable reinforcement. The domain of influence for the nodes close to the interface in either patch is truncated. Therefore, nodes in the same patch can only influence points included in each patch. The stiffness matrix is constructed in each patch, respectively. The constraint condition to impose continuous displacement at the interface is given as follows:

$$\left(\phi_I^1(\mathbf{x}_d)-\phi_I^2(\mathbf{x}_d)\right)\mathbf{u}_I=0 \tag{6}$$

where ϕ_I^1 and ϕ_I^2 are approximation functions obtained by MLSA from patch 1 and 2 and $\mathbf{x}_d$ is a position vector at the interface. The whole stiffness matrix $\mathbf{K}^*$ is obtained by the assemblage of each stiffness with the penalty term, as

$$\mathbf{K}_{IJ}^*=\mathbf{K}_{IJ}^1+\mathbf{K}_{IJ}^2+\alpha\int_{\Gamma_s}\left(\phi_I^1(\mathbf{x}_d)\phi_J^1(\mathbf{x}_d)-\phi_I^2(\mathbf{x}_d)\phi_J^2(\mathbf{x}_d)\right)\,d\Gamma_s \tag{7}$$

where α is a penalty number, $\mathbf{K}^1$, $\mathbf{K}^2$ are the stiffness matrices obtained from each patch and Γ_s is the interface of patch.

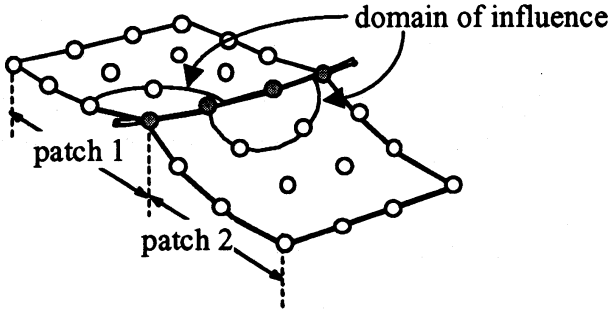

Fig.1: Domain of influence close to the interface of patch

Arbitrary Lagrangian Eulerian Formulation in EFGM

For analyzing moving discontinuity caused by a sliding cable, the boundary of patch must be coincided with the discontinuous line of slope. In the proposed ALE formulation, the displacement of membrane structure and the sliding of cable on membrane surface are treated as different variable.

In the formulation based on ALE method, both the initial configuration ${}^t\mathbf{X}$ and the current configuration ${}^t\mathbf{x}$ are treated as unknown variables. Each coordinate is described by using an arbitrary spatial reference configuration x^r as follows:

$${}^t\mathbf{X}=\mathbf{X}(x^r,\ t) \tag{8}$$

$$ {}^{t}\mathbf{X} = \mathbf{X}(x^{r},\ t) \tag{9} $$

and its displacement ${}^{t}\mathbf{u}$ is

$$ {}^{t}\mathbf{u} = \mathbf{u}(x^{r},\ t) = {}^{t}\mathbf{x} - {}^{t}\mathbf{X}. \tag{10} $$

The total displacement is separated into the Eulerian displacement ${}^{t}\bar{\mathbf{u}}$ and the Lagrangian displacement ${}^{t}\hat{\mathbf{u}}$.

$$ {}^{t}\mathbf{u} = {}^{t}\bar{\mathbf{u}} + {}^{t}\hat{\mathbf{u}} \tag{11} $$

$$ {}^{t}\mathbf{X} = {}^{0}\mathbf{X} - {}^{t}\bar{\mathbf{u}} \tag{12} $$

$$ {}^{t}\hat{\mathbf{x}} = {}^{0}\hat{\mathbf{x}} + {}^{t}\hat{\mathbf{u}} \tag{13} $$

In the analysis, the Eulerian displacement shows the flow of material point in the initial configuration and the Lagrangian displacement shows the displacements of nodes. The deformation gradient tensor of total displacement ${}^{t}\mathbf{F}$ can be written in the index form as,

$$ {}^{t}F_{ij} = \frac{\partial\, {}^{t}x_i}{\partial\, {}^{t}X_j} = \frac{\partial\, {}^{t}x_i}{\partial x_k^{r}} \frac{\partial x_k^{r}}{\partial\, {}^{t}X_j} = {}^{t}\hat{F}_{ik}\, {}^{t}\bar{F}_{kj} \tag{14} $$

and is also separated into the Eulerian and the Lagrangian parts, too.

$$ {}^{t}\bar{F}_{ij} = \frac{\partial x_i^{r}}{\partial\, {}^{t}X_j} = ({}^{t}\tilde{F}_{ij})^{-1},\ {}^{t}\tilde{F}_{ij} = \frac{\partial\, {}^{t}X_i}{\partial x_j^{r}} \tag{15} $$

$$ {}^{t}\hat{F}_{ij} = \frac{\partial\, {}^{t}x_i}{\partial x_j^{r}} \tag{16} $$

The Eularian ${}^{t}\bar{\mathbf{F}}$ describes the mapping from ^{t} the initial to the reference configuration and the Lagrangian ${}^{t}\hat{\mathbf{F}}$ describes the mapping from the reference to the current configuration. The concept of ALE formulation is illustrated in Fig.2[5].

The components of the Green-Lagrange strain tensor is written as

$$ {}^{t}E_{ij} = \frac{1}{2}\left[{}^{t}F_{ki}\, {}^{t}F_{kj} - \delta_{ij}\right] = \frac{1}{2}\left[{}^{t}\hat{F}_{ki}\, {}^{t}\hat{F}_{km}\, {}^{t}\bar{F}_{li}\, {}^{t}\bar{F}_{mj} - \delta_{ij}\right] \tag{17} $$

where δ_{ij} is the Kronecker delta.
Then, the total potential energy in the reference configuration is shown.

$$ {}^{t}\Pi = \frac{1}{2}\int_{v} {}^{t}\mathbf{S} : {}^{t}\mathbf{E}\, {}^{t}\tilde{J}\, dv^{r} - \int_{v} ({}^{t}\hat{\mathbf{u}} + {}^{t}\bar{\mathbf{u}}) \cdot {}^{t}\mathbf{b}\, {}^{t}\tilde{J}\, dv^{r} + \frac{1}{2}\alpha\int_{\Gamma_L} ({}^{t}\hat{\mathbf{u}} - {}^{t}\underline{\hat{\mathbf{u}}})^{2} d\Gamma_{L} + \frac{1}{2}\alpha\int_{\Gamma_E} ({}^{t}\bar{\mathbf{u}} - {}^{t}\underline{\bar{\mathbf{u}}})^{2} d\Gamma_{E} \tag{18} $$

where v^{r} is the volume in reference configuration, Γ_L and Γ_E are boundaries for Lagrangian and Eulerian displacement, ${}^{t}\underline{\hat{\mathbf{u}}}$ and ${}^{t}\underline{\bar{\mathbf{u}}}$ are prescribed displacements at each boundary and ${}^{t}\tilde{J}$ is volume ratio from reference configuration to initial configuration calculated from the determinant of the inverse Eulerian deformation gradient.

$$\int_{{}^{t}V} d\,{}^{t}V = \int_{V^r} \left| \frac{\partial\, {}^{t}\mathbf{X}}{\partial x^r} \right| dv^r = \int_{V^r} {}^{t}\tilde{J}\, dv^r \tag{19}$$

$${}^{t}\tilde{J} = \varepsilon_{ijk}\, {}^{t}\tilde{F}_{i1}\, {}^{t}\tilde{F}_{j2}\, {}^{t}\tilde{F}_{k3} \tag{20}$$

where, ${}^{t}V$ is the initial volume.

From the variation of eq.(18) with respect to Lagrangian and Eulerian displacement, eq.(21) is obtained which is equivalent to the virtual work principle.

$$\begin{aligned} &\int_{V^r} \left\{ {}^{t}\mathbf{S} : \delta\, {}^{t}\mathbf{E}\, {}^{t}\tilde{J} + \frac{1}{2}\, {}^{t}\mathbf{S} : {}^{t}\mathbf{E}\, \delta\, {}^{t}\tilde{J} \right\} dv^r - \int_{V^r} (\delta\hat{\mathbf{u}} + \delta\bar{\mathbf{u}}) \cdot {}^{t}\mathbf{b}\, {}^{t}\tilde{J} + ({}^{t}\hat{\mathbf{u}} + {}^{t}\bar{\mathbf{u}}) \cdot {}^{t}\mathbf{b}\, \delta\tilde{J}\, dv^r \\ &+\alpha \int_{\Gamma_L} \delta\hat{\mathbf{u}} \cdot ({}^{t}\hat{\mathbf{u}} - {}^{t}\underline{\hat{\mathbf{u}}})\, d\Gamma_L + \alpha \int_{\Gamma_E} \delta\bar{\mathbf{u}} \cdot ({}^{t}\bar{\mathbf{u}} - {}^{t}\underline{\bar{\mathbf{u}}})\, d\Gamma_E = 0 \end{aligned} \tag{21}$$

This stiffness equation is nonlinear in general, so we introduce the linearized incremental expression for eq.(21).

$$\begin{aligned} &\int_{V^r} \left\{ ({}^{t}\mathbf{S} + \mathbf{S}) : (\delta\mathbf{E}_L + \delta\mathbf{E}_{NL})({}^{t}\tilde{J} + \tilde{J}) + \frac{1}{2}({}^{t}\mathbf{S} + \mathbf{S}) : ({}^{t}\mathbf{E} + \mathbf{E})(\delta\tilde{J}_L + \delta\tilde{J}_{NL}) \right\} dv^r \\ &- \int_{V^r} (\delta\hat{\mathbf{u}} + \delta\bar{\mathbf{u}}) \cdot {}^{t}\mathbf{b}({}^{t}\tilde{J} + \tilde{J})\, dv^r - \int_{V^r} ({}^{t}\hat{\mathbf{u}} + {}^{t}\bar{\mathbf{u}}) \cdot {}^{t}\mathbf{b}(\delta\tilde{J}_L + \delta\tilde{J}_{NL})\, dv^r \\ &+\alpha \int_{\Gamma_L} \delta\hat{\mathbf{u}} \cdot ({}^{t}\hat{\mathbf{u}} - {}^{t}\underline{\hat{\mathbf{u}}})\, d\Gamma_L + \alpha \int_{\Gamma_E} \delta\bar{\mathbf{u}} \cdot ({}^{t}\bar{\mathbf{u}} - {}^{t}\underline{\bar{\mathbf{u}}})\, d\Gamma_E = 0 \end{aligned} \tag{22}$$

In eq.(22), the variables without superscript show increment from time t to time t+Δt, and eqs.(23) and (24) are utilized to derive eq.(22).

$$\delta\, {}^{t+\Delta t}\mathbf{E} = \delta\mathbf{E} = \delta\mathbf{E}_L + \delta\mathbf{E}_{NL} \tag{23}$$

$$\delta\, {}^{t+\Delta t}\tilde{J} = \delta\tilde{J} = \delta\tilde{J}_L + \delta\tilde{J}_{NL} \tag{24}$$

where $_L$ and $_{NL}$ are linear and quadratic terms, respectively. And then, $\tilde{J}$ is given by

$${}^{t+\Delta t}\tilde{\mathbf{F}} = \frac{\partial\, {}^{t}\mathbf{X}}{\partial x^r} - \frac{\partial \bar{\mathbf{u}}}{\partial x^r} \tag{25}$$

$$\begin{aligned} \tilde{J} = &-\varepsilon_{ijk} \left(\frac{\partial \bar{u}_i}{\partial x^r{}_1} \frac{\partial\, {}^{t}X_j}{\partial x^r{}_2} \frac{\partial\, {}^{t}X_k}{\partial x^r{}_3} + \frac{\partial\, {}^{t}X_i}{\partial x^r{}_1} \frac{\partial \bar{u}_j}{\partial x^r{}_2} \frac{\partial\, {}^{t}X_k}{\partial x^r{}_3} + \frac{\partial\, {}^{t}X_i}{\partial x^r{}_1} \frac{\partial\, {}^{t}X_j}{\partial x^r{}_2} \frac{\partial \bar{u}_k}{\partial x^r{}_3} \right) \\ &+\varepsilon_{ijk} \left(\frac{\partial \bar{u}_i}{\partial x^r{}_1} \frac{\partial \bar{u}_j}{\partial x^r{}_2} \frac{\partial\, {}^{t}X_k}{\partial x^r{}_3} + \frac{\partial \bar{u}_i}{\partial x^r{}_1} \frac{\partial\, {}^{t}X_j}{\partial x^r{}_2} \frac{\partial \bar{u}_k}{\partial x^r{}_3} + \frac{\partial\, {}^{t}X_i}{\partial x^r{}_1} \frac{\partial \bar{u}_j}{\partial x^r{}_2} \frac{\partial \bar{u}_k}{\partial x^r{}_3} \right) \\ &-\varepsilon_{ijk} \frac{\partial \bar{u}_i}{\partial x^r{}_1} \frac{\partial \bar{u}_j}{\partial x^r{}_2} \frac{\partial \bar{u}_k}{\partial x^r{}_3} \end{aligned} \tag{26}$$

Eq.(22) is rewritten as Eq.(27).

$$
\begin{aligned}
&\int_V \left\{ ({}^t\mathbf{S}:\delta\mathbf{E}_L\tilde{J} + {}^t\mathbf{S}:\delta\mathbf{E}_{NL}{}^t\tilde{J} + \mathbf{S}:\delta\mathbf{E}_L{}^t\tilde{J}) + \frac{1}{2}({}^t\mathbf{S}:{}^t\mathbf{E}\delta\tilde{J}_{NL} + {}^t\mathbf{S}:\mathbf{E}\delta\tilde{J}_L + \mathbf{S}:{}^t\mathbf{E}\delta\tilde{J}_L) \right\} dV \\
&\quad - \int_V \left\{ (\delta\hat{\mathbf{u}} + \delta\bar{\mathbf{u}}) \cdot {}^t\mathbf{b}\tilde{J} + ({}^t\hat{\mathbf{u}} + {}^t\bar{\mathbf{u}}) \cdot {}^t\mathbf{b}\delta\tilde{J}_{NL} + (\hat{\mathbf{u}} + \bar{\mathbf{u}}) \cdot {}^t\mathbf{b}\delta\tilde{J}_L \right\} dV \\
&\quad + \alpha \int_{\Gamma_L} \delta\hat{\mathbf{u}} \cdot \hat{\mathbf{u}} d\Gamma_L + \alpha \int_{\Gamma_E} \delta\bar{\mathbf{u}} \cdot \bar{\mathbf{u}} d\Gamma_E \\
&= \int_V \left\{ (\delta\hat{\mathbf{u}} + \delta\bar{\mathbf{u}}) \cdot {}^t\mathbf{b}{}^t\tilde{J} + ({}^t\hat{\mathbf{u}} + {}^t\bar{\mathbf{u}}) \cdot {}^t\mathbf{b}\delta\tilde{J}_L \right\} dV - \int_V \left\{ {}^t\mathbf{S}:\delta\mathbf{E}_L{}^t\tilde{J} + \frac{1}{2}{}^t\mathbf{S}:{}^t\mathbf{E}\delta\tilde{J}_L \right\} dV \\
&\quad - \alpha \int_{\Gamma_L} \delta\hat{\mathbf{u}} \cdot ({}^t\hat{\mathbf{u}} - {}^{t'}\underline{\hat{\mathbf{u}}}) d\Gamma_L - \alpha \int_{\Gamma_E} \delta\bar{\mathbf{u}} \cdot ({}^t\bar{\mathbf{u}} - {}^{t'}\underline{\bar{\mathbf{u}}}) d\Gamma_E
\end{aligned}
\tag{27}
$$

Each displacement fields are discretized using shape function calculated by MLSA.

$$\hat{\mathbf{u}}(\mathbf{x}) = \phi_I(\mathbf{x})\hat{\mathbf{u}}_I \tag{28}$$

$$\bar{\mathbf{u}}(\mathbf{x}) = \phi_I(\mathbf{x})\bar{\mathbf{u}}_I \tag{29}$$

By solving eq.(27) using iterative solution like Newton-Raphson method, the analysis considering sliding can be conducted.

In case of the analysis considering friction, the next term is added to the left side of eq.(22).

$$-\int_{\Gamma_F} \delta\bar{\mathbf{u}} \cdot {}^t\mathbf{f} d\Gamma_F \tag{30}$$

where, ${}^t\mathbf{f}$ means friction force and Γ_F is the area where friction works. Friction works on only the Euler displacement.

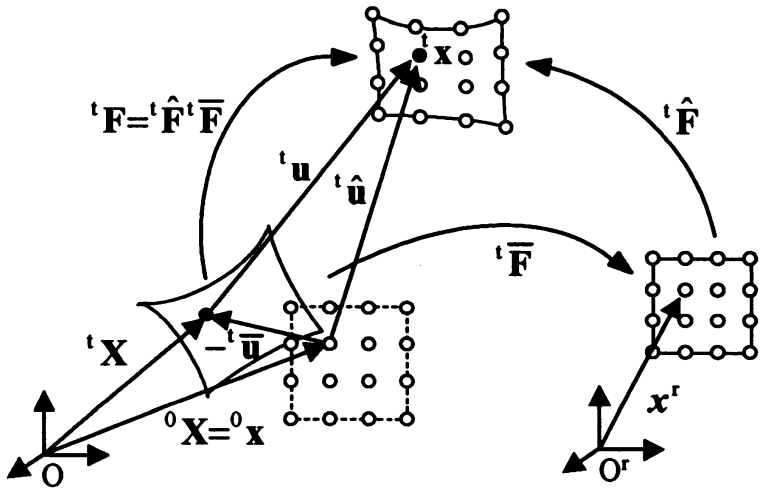

Fig.2: Concept of ALE method

Numerical Example

A simple problem is analyzed to verify the proposed formulation. Figure 3 shows an analysis model of membrane on frictionless pulley. Membrane is fixed at the both ends, passes over a frictionless roller that

can move horizontally. The Young's modulus is $1.0x10^6$, and Poisson's ratio is zero. The number of nodes is 25 in each patch. This structure is subjected to a horizontal load at the roller and the load is equally distributed on the nodes at the roller.

The deformed shape is shown in Fig.4. The x-direction displacement for the roller was –0.20889, and the Eulerian displacement was 0.1298. Eulerian displacements show the slip displacements.

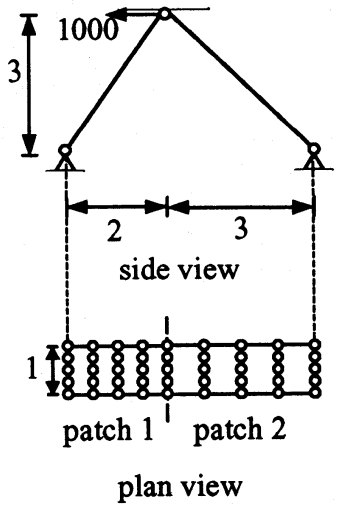

Fig.3: Analysis model

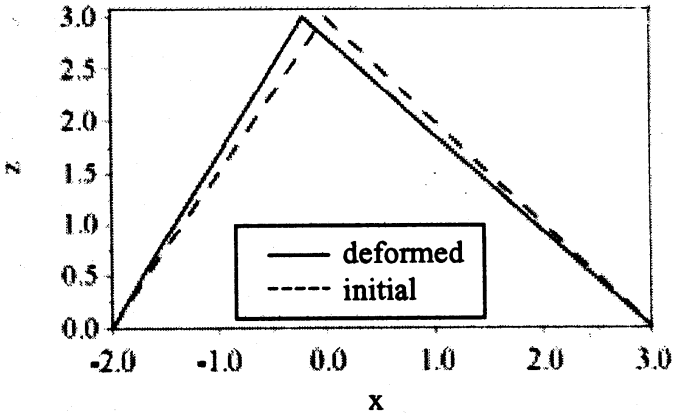

Fig.4: Analysis result

Figure 5 shows an analysis model of a membrane structure represented by bi-quadratic function. The arrangement of nodes is shown in Fig.6. This model is separated two patches at x=0, and the number of nodes at one patch is 6x11. The radius of the domain of influence is 1.1c. The section stiffness Eh is equal to $6.0x10^6$ N/m, where h denotes the thickness, and the Poisson's ratio is 0.267. The Lagrangian displacement is fixed along line x=0, because of the tensed cable for reinforcement. 'Eulerian nodes' in Fig.6 show the location of fixed cable, so they have only the Eulerian displacement. The Eulerian displacement shows the slide between the cable and the membrane surface. In this analysis, the effect of friction is not taken into account for brevity.

The pressure load $5.0x10^5$ Pa is applied to z-direction only for patch2. Then, the analysis result under the condition that the cable is fixed on the membrane ($\bar{\mathbf{u}}$=0) is compared with the case that the cable is free from the membrane ($\bar{\mathbf{u}}$:free).

The configuration along line y=0 after deformation on each condition is shown in Fig. 7. In the case of that the cable slides on the membrane, the right side of membrane is more swelled and the left side becomes straight. The locations of nodes on the cable are coincided in each condition, therefore, the movement of only material point can be represented.

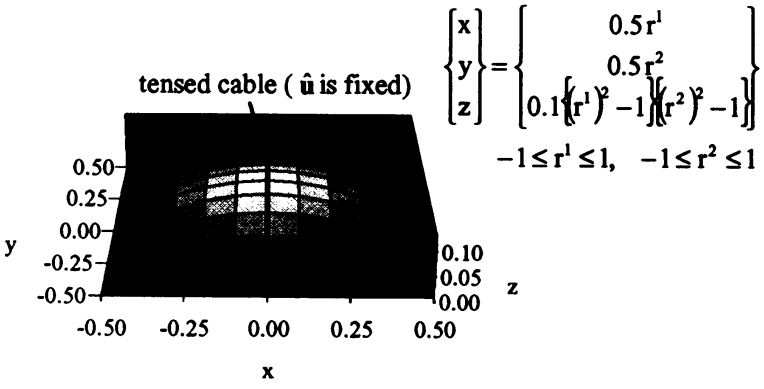

Fig.5: Analysis model

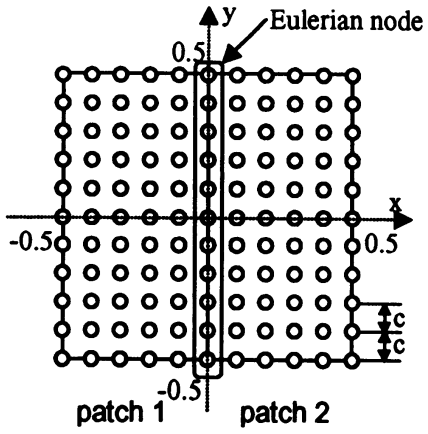

Fig.6: Nodal arrangement

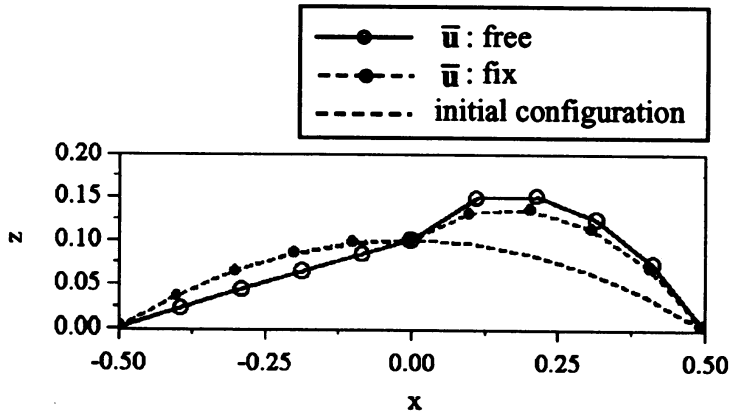

Fig.7: Configuration after deformation along line y=0

Conclusion

In this paper, ALE based EFGM formulation considering slide and friction is proposed and applied to the analysis of membrane structure with sliding cable. Additionally, by using patch technique, discontinuous slope of membrane surface can be represented. In future research, the analysis fully taking account of the effect of friction should be conducted.

References

1. Belytschko, T., Lu, Y. Y. and Gu, L. (1994): "Element Free Galerkin Methods", *International Journal for Numerical Methods in Engineering*, Vol. 37, pp. 229-256.
2. Kawashima, T. and Noguchi, H. (1999): "The Analyses of Membrane Structures with Cable Reinforcement by Element Free Method", *Proceedings of Fourth Asia-Pacific Conference on Computational Mechanics*, Vol.2, pp. 1003-1008.
3. Cordes, W. and Moran, B. (1996): "Treatment of Material Discontinuity in the Element-Free Galerkin Method", *Computer Methods in Applied Mechanics and Engineering*, Vol. 139, pp. 75-89.
4. Haber, R. B. (1984): "A Mixed Eulerian-Lagrangian Displacement Model for Large-Deformation Analysis in Solid Mechanics", *Computer Methods in Applied Mechanics and Engineering*, Vol. 43, pp. 277-292.
5. Haber, R. B. et.al. (1983): "Contact-Slip Analysis using Mixed Displacements", *Journal of Engineering Mechanics*, Vol. 109, No. 2, pp. 411-429.